International Journal of Information, Control and Computer Sciences
ISSN: 2517-9942
Vol:5, No:12, 2011

Active and Reactive Power Control of a DFIG with MPPT for Variable Speed Wind Energy Conversion using Sliding Mode Control

Youcef Bekakra, Djilani Ben attous

Abstract—This paper presents the study of a variable speed wind energy conversion system based on a Doubly Fed Induction Generator (DFIG) based on a sliding mode control applied to achieve control of active and reactive powers exchanged between the stator of the DFIG and the grid to ensure a Maximum Power Point Tracking (MPPT) of a wind energy conversion system. The proposed control algorithm is applied to a DFIG whose stator is directly connected to the grid and the rotor is connected to the PWM converter. To extract a maximum of power, the rotor side converter is controlled by using a stator flux-oriented strategy. The created decoupling control between active and reactive stator power allows keeping the power factor close to unity. Simulation results show that the wind turbine can operate at its optimum energy for a wide range of wind speed.

Keywords—Doubly fed induction generator, wind energy, wind turbine, sliding mode control, maximum power point tracking (MPPT).

I. Introduction

THE most important advantages of the variable speed wind turbines as compared with conventional constant speed system are the improved dynamic behavior, resulting in the reduction of the drive train mechanical stress and electrical power fluctuation, and also the increase of power capture. One of the generation systems commercially available in the wind energy market currently is the doubly fed induction generator (DFIG) with its stator winding directly connected to the grid and with its rotor winding connected to the grid through a variable frequency converter as shown in Fig. 1. One of the most advantages of this system is that the rating of the power converter is one third of that of the generator [1].

The doubly fed induction generator is widely used for variable-speed generation, and it is one of the most important generators for wind energy conversion systems. Both grid connected and stand-alone operation is feasible [2].

The variable speed constant frequency (VSCF) wind power generation is mainly based on the research of optimal power-speed curve, namely the most mechanical power of turbine can be achieved by regulating the speed of generator, where the wind speed may be detected or not [1].

Through studying the characteristics of wind turbine, the paper used the maximum power point tracking (MPPT) control process. Firstly, according to the DFIG character, the paper adopts the vector transformation control method of stator oriented magnetic field to realize the decoupling control for the active power and reactive power using sliding mode control (SMC).

Sliding mode theory, stemmed from the variable structure control family, has been used for the induction motor drive for a long time. It has for long been known for its capabilities in accounting for modelling imprecision and bounded disturbances. It achieves robust control by adding a discontinuous control signal across the sliding surface, satisfying the sliding condition. Nevertheless, this type of control has an essential drawback, which is the chattering phenomenon caused from the discontinuous control action. To alleviate the chattering phenomenon, the idea of boundary layer is used to improve it. It is called a modified controller. In this method, the control action was smoothed such that the chattering phenomenon can be decreased [3].

In this paper, we apply the SMC method to the wind energy conversion systems with MPPT control algorithm.

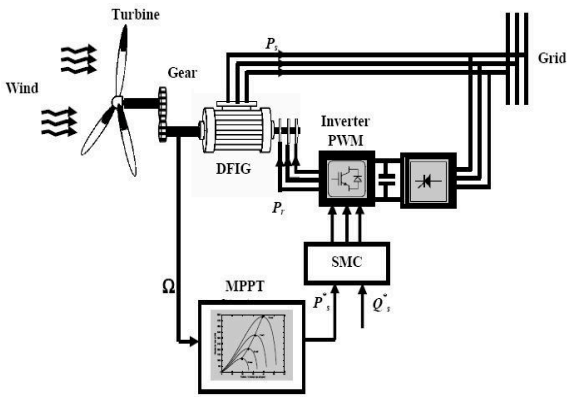

Fig. 1. DFIG variable speed wind energy conversion MPPT control

II. MODEL OF TURBINE

The wind turbine input power usually is [4]:

$$P_v = \frac{1}{2}\rho S_\omega v^3 \quad (1)$$

Where ρ is air density; S_ω is wind turbine blades swept area in the wind; v is wind speed.
The output mechanical power of wind turbine is:

$$P_m = C_p P_v = \frac{1}{2} C_p \rho S_\omega v^3 \quad (2)$$

Department of Electrical Engineering, El-Oued University Center, Algeria. e-mail: (youcef1984@gmail.com, dbenattous@yahoo.com).

Where C_p represents the wind turbine power conversion efficiency. It is a function of the tip speed ratio λ and the blade pitch angle β in a pitch-controlled wind turbine. $\lambda$is defined as the ratio of the tip speed of the turbine blades to wind speed:

$$\lambda = \frac{R.\Omega_t}{v} \tag{3}$$

Where R is blade radius, Ω_t is angular speed of the turbine.

C_p can be described as [5]:

$$C(\beta,\lambda) = (0.5 - 0.0167.(\beta - 2)).\sin(\frac{\pi.(\lambda+0.1)}{18.5-0.3.(\beta-2)}) \\ -0.00184.(\lambda-3)(\beta-2) \tag{4}$$

A figure showing the relation between C_p, β and λ is shown in Fig. 2. The maximum value of $C_p(C_{p\_max} = 0.5)$ is achieved for $\beta = 2$ degree and for $\lambda_{optim} = 9.2$.

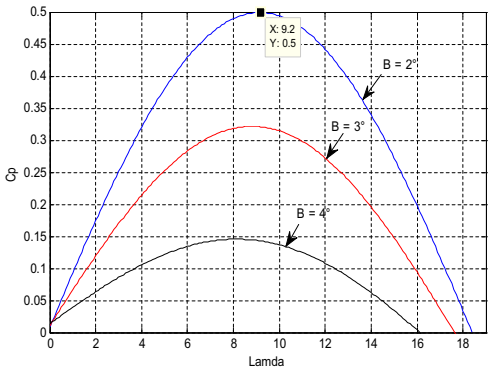

Fig. 2. Aerodynamic power coefficient variation C_p against tip speed ratio λ and pitch angle β

III. MAXIMUM POWER POINT TRACKING (MPPT)

Maximum power variation with rotation speed Ω of DFIG is predefined for each wind turbine. So for MPPT, the control system should follow the tracking characteristic curve (TCC) of the wind turbine [6]. Each wind turbine has TCC similar to the one shown in Fig. 3. The actual wind turbine, Ω is measured and the corresponding mechanical power of the TCC is used as the reference power for the power control loop [6].

In order to make full use of wind energy, in low wind speed β should be equal to 2 degree. Fig. 3 illustrates the wind turbine power curve when β is equal to 2 degree.

To extract the maximum power generated, we must fix the advance report λ_{optim} is the maximum power coefficient C_{p_max} , the measurement of wind speed is difficult, an estimate of its value can be obtained :

$$v_{est} = \frac{R.\Omega_t}{\lambda_{optim}} \tag{5}$$

The aerodynamic power reference value must be set to the following value:

$$P_{aer\_ref} = \frac{1}{2} C_{p\_max} \rho S_\omega v_{est}^3 \tag{6}$$

From figure 2 we can see there is one specific angular frequency at which the output power of wind turbine is maximum occurs at the point where C_p is maximized. Connected all the maximum power point of each power curve, the optimal power curve (MPPT curve) is obtained.

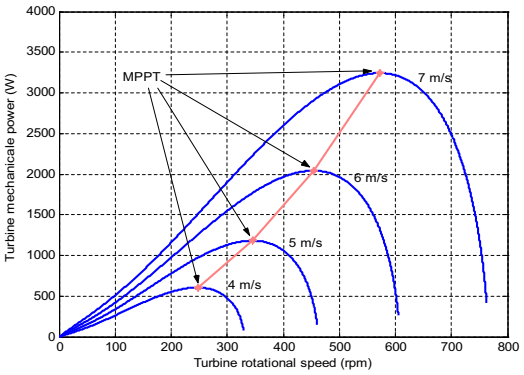

Fig. 3. Turbine powers various speed characteristics for different wind speeds, with indication of the maximum power tracking curve

IV. MODELING OF THE DFIG

The general electrical state model of the induction machine obtained using Park transformation is given by the following equations [7]:

Stator and rotor voltages:

$$\begin{cases} V_{sd} = R_s i_{sd} + \frac{d}{dt}\phi_{sd} - \omega_s \phi_{sq} \\ V_{sq} = R_s i_{sq} + \frac{d}{dt}\phi_{sq} + \omega_s \phi_{sd} \\ V_{rd} = R_r i_{rd} + \frac{d}{dt}\phi_{rd} - (\omega_s - \omega)\phi_{rq} \\ V_{rq} = R_r i_{rq} + \frac{d}{dt}\phi_{rq} + (\omega_s - \omega)\phi_{rd} \end{cases} \tag{7}$$

Stator and rotor fluxes:

$$\begin{cases} \phi_{sd} = L_s i_{sd} + M i_{rd} \\ \phi_{sq} = L_s i_{sq} + M i_{rq} \\ \phi_{rd} = L_r i_{rd} + M i_{sd} \\ \phi_{rq} = L_r i_{rq} + M i_{sq} \end{cases} \tag{8}$$

The electromagnetic torque is given as:

$$C_e = pM(i_{rd} i_{sq} - i_{rq} i_{sd}) \tag{9}$$

and its associated motion equation is:

$$C_e - C_r = J\frac{d\Omega}{dt} \tag{10}$$

The state variable vector is then :

$$X = \left[\begin{array}{cccc} i_{sd} & i_{sq} & i_{rd} & i_{rq} \end{array} \right]^T$$

The state model can then be written as :

$$\dot{X} = A.X + B.U \tag{11}$$

With :

$$\dot{X} = \left[\begin{array}{cccc} \frac{d}{dt}i_{sd} & \frac{d}{dt}i_{sq} & \frac{d}{dt}i_{rd} & \frac{d}{dt}i_{rq} \end{array} \right]^T$$

$$U = \left[\begin{array}{cccc} V_{sd} & V_{sq} & V_{rd} & V_{rq} \end{array} \right]^T$$

$$A = \left[\begin{array}{cccc} -a_1 & a\omega + \omega_s & a_3 & a_5\omega \\ -a\omega - \omega_s & -a_1 & -a_5\omega & a_3 \\ a_4 & -a_6\omega & -a_2 & -\frac{\omega}{\sigma} + \omega_s \\ a_6\omega & a_4 & \frac{\omega}{\sigma} - \omega_s & \end{array} \right],$$

$$B = \left[\begin{array}{cccc} b_1 & 0 & -b_3 & 0 \\ 0 & b_1 & 0 & -b_3 \\ -b_3 & 0 & b_2 & 0 \\ 0 & -b_3 & 0 & b_2 \end{array} \right]$$

Where:

$a = \frac{1-\sigma}{\sigma}$, $a_1 = \frac{R_s}{\sigma L_s}$, $a_2 = \frac{R_r}{\sigma L_r}$, $a_3 = \frac{R_r M}{\sigma L_s L_r}$,

$a_4 = \frac{R_s M}{\sigma L_s L_r}$, $a_5 = \frac{M}{\sigma L_s}$, $a_6 = \frac{M}{\sigma L_r}$, $b_1 = \frac{1}{\sigma L_s}$,

$b_2 = \frac{1}{\sigma L_r}$, $b_3 = \frac{M}{\sigma L_s L_r}$.

V. Field oriented control of DFIG

In this section, the DFIM model can be described by the following state equations in the synchronous reference frame whose axis d is aligned with the stator flux vector, ($\phi_{sd} = \phi_s$ and $\phi_{sq} = 0$).

The control of the DFIG must allow a control independent of the active and reactive powers by the rotor voltages generated by an inverter.

By choosing a reference frame linked to the stator flux and if the per phase stator resistance is neglected, which is a realist approximation for medium and high power machines used in wind energy conversion, the stator voltage vector is consequently in quadrature advance in comparison with the stator flux vector [7]:

$$V_{sd} = 0 \quad and \quad V_{sq} = V_s \approx \omega_s.\phi_s \tag{12}$$

We lead to an uncoupled power control; where, the transversal component i_{rq} of the rotor current controls the active power. The reactive power is imposed by the direct component i_{rd}.

$$P_s = -V_s\frac{M}{L_s}i_{rq} \tag{13}$$

$$Q_s = \frac{V_s^2}{\omega_s L_s} - V_s\frac{M}{L_s}i_{rd} \tag{14}$$

The arrangement of the equations gives the expressions of the voltages according to the rotor currents:

$$\dot{i_{rd}} = -\frac{1}{\sigma T_r}i_{rd} + g\omega_s i_{rq} + \frac{1}{\sigma L_r}V_{rd} \tag{15}$$

$$\dot{i_{rq}} = -(\frac{1}{T_r} + \frac{M^2}{L_s T_s L_r})\frac{1}{\sigma}i_{rq} - g\omega_s i_{rd} + \frac{1}{\sigma L_r}V_{rq} \tag{16}$$

With:

$T_r = \frac{L_r}{R_r}$, $T_s = \frac{L_s}{R_s}$, $g = \frac{\omega_s - \omega}{\omega_s}$, $\sigma = 1 - \frac{M^2}{L_s L_r}$.

VI. Sliding mode control

A Sliding Mode Controller (SMC) is a Variable Structure Controller (VSC). Basically, a VSC includes several different continuous functions that can map plant state to a control surface, whereas switching among different functions is determined by plant state represented by a switching function [8].

The design of the control system will be demonstrated for a following nonlinear system [9]:

$$\dot{x} = f(x,t) + B(x,t).u(x,t) \tag{17}$$

Where $x \in \Re^n$ is the state vector, $f(x,t) \in \Re^n$, $B(x,t) \in \Re^{n\times m}$, $u \in \Re^m$ is the control vector.

From the system (17), it possible to define a set S of the state trajectories x such as:

$$S = \{x(t) | \sigma(x,t) = 0\} \tag{18}$$

Where:

$$\sigma(x,t) = [\sigma_1(x,t), \sigma_2(x,t), ..., \sigma_m(x,t)]^T \tag{19}$$

and $[.]^T$ denotes the transposed vector, S is called the sliding surface.

To bring the state variable to the sliding surfaces, the following two conditions have to be satisfied:

$$\sigma(x,t) = 0, \dot{\sigma(x,t)} = 0 \tag{20}$$

The control law satisfies the precedent conditions is presented in the following form:

$$\left\{ \begin{array}{l} u = u^{eq} + u^n \\ u^n = -k_f.sgn(\sigma(x,t)) \end{array} \right. \tag{21}$$

Where u is the control vector, u^{eq} is the equivalent control vector, u^n is the switching part of the control (the correction factor), k_f is the controller gain. u^{eq} can be obtained by considering the condition for the sliding regimen, $\sigma(x,t)$. The equivalent control keeps the state variable on sliding surface, once they reach it.

For a defined function [10], [11]:

$$sgn(\phi) = \begin{cases} 1\ , & if \quad \phi>0 \\ 0\ , & if \quad \phi=0 \\ -1\ , & if \quad \phi<0 \end{cases} \tag{22}$$

The controller described by the equation (21) presents high robustness, insensitive to parameter fluctuations and disturbances, but it will have high-frequency switching (chattering phenomena) near the sliding surface due to sgn function involved. These drastic changes of input can be avoided by introducing a boundary layer with width ε [9]. Thus replacing $sgn(\sigma(t)/\varepsilon)$ by $sat(\sigma(t)/\varepsilon)$ (saturation function), in (21), we have:

$$u = u^{eq} - k_f.sat(\sigma(x,t)) \tag{23}$$

Where, $\varepsilon > 0$

$$sat(\phi) = \begin{cases} sgn(\phi)\ , & if \quad |\phi| \geq 0 \\ \phi \quad , & if \quad |\phi| < 0 \end{cases} \tag{24}$$

Consider a Lyapunov function [10]:

$$V = \frac{1}{2}\sigma^2 \tag{25}$$

From Lyapunov theorem we know that if $\dot{V}$ is negative definite, the system trajectory will be driven and attracted toward the sliding surface and remain sliding on it until the origin is reached asymptotically [9]:

$$V = \frac{1}{2}\frac{d}{dt}\sigma^2 = \sigma\dot{\sigma} \leq -\eta|\sigma| \tag{26}$$

Where η is a strictly positive constant.

In this paper, we use the sliding surface proposed par J.J. Slotine:

$$\sigma(x,t) = (\frac{d}{dt} + \tau)^{n-1}.e \tag{27}$$

Where:

$x = [x, \dot{x}, ..., x^{n-1}]^T$ is the state vector,

$x_d = [x_d, \dot{x_d}, ..., x_d^{n-1}]^T$ is the desired state vector,

$e = [e, \dot{e}, ..., e^{n-1}]^T$ is the error vector, and τ is a positive coefficient, and n is the system order.

Commonly, in DFIM control using sliding mode theory, the surfaces are chosen as functions of the error between the reference input signal and the measured signals [9].

VII. Application of Sliding Mode Control to DFIG

The rotor currents (which are linked to active and reactive powers by equations (13) and (14), quadrature rotor current i_{rq} linked to stator active power P_s and direct rotor current i_{rd} linked to stator reactive power Q_s) have to track appropriate current references, so, a sliding mode control based on the above Park reference frame is used.

A. Quadrature rotor current control with SMC

The sliding surface representing the error between the measured and reference quadrature rotor current is given by this relation:

$$e = i_{rq}^* - i_{rq} \tag{28}$$

For $n = 1$, the speed control manifold equation can be obtained from equation (27) as follow:

$$\sigma(i_{rq}) = e = i_{rq}^* - i_{rq} \tag{29}$$

$$\dot{\sigma}(i_{rq}) = \dot{i_{rq}^*} - \dot{i_{rq}} \tag{30}$$

Substituting the expression of $\dot{i_{rq}}$ equation (16) in equation (30), we obtain:

$$\dot{\sigma}(i_{rq}) = \dot{i_{rq}^*} - (-\frac{1}{\sigma}(\frac{1}{T_r} + \frac{M^2}{L_s T_s L_r})i_{rq} - g\omega_s i_{rd} + \frac{1}{\sigma L_r}V_{rq}) \tag{31}$$

We take:

$$V_{rq} = V_{rq}^{eq} + V_{rq}^n \tag{32}$$

During the sliding mode and in permanent regime, we have:

$$\sigma(i_{rq}) = 0,\ \ \dot{\sigma}(i_{rq}) = 0,\ \ V_{rq}^n = 0$$

Where the equivalent control is:

$$V_{rq}^{eq} = (\dot{i_{rq}^*} + \frac{1}{\sigma}(\frac{1}{T_r} + \frac{M^2}{L_s T_s L_r})i_{rq} + g\omega_s i_{rd})\sigma L_r \tag{33}$$

Therefore, the correction factor is given by:

$$V_{rq}^n = k_{V_{rq}}.sat(\sigma(i_{rq})) \tag{34}$$

$k_{V_{rq}}$: positive constant.

B. Direct rotor current control with SMC:

The sliding surface representing the error between the measured and reference direct rotor current is given by this relation:

$$e = i_{rd}^* - i_{rd} \tag{35}$$

For $n = 1$, the speed control manifold equation can be obtained from equation (27) as follow:

$$\sigma(i_{rd}) = e = i_{rd}^* - i_{rd} \tag{36}$$

$$\dot{\sigma}(i_{rd}) = \dot{i_{rd}^*} - \dot{i_{rd}} \tag{37}$$

Substituting the expression of $\dot{i_{rd}}$ equation (15) in equation (37), we obtain:

$$\dot{\sigma}(i_{rd}) = \dot{i_{rd}^*} - (-\frac{1}{\sigma T_r} i_{rd} + g\omega_s i_{rq} + \frac{1}{\sigma L_r} + V_{rd}) \tag{38}$$

We take:

$$V_{rd} = V_{rd}^{eq} + V_{rd}^{n} \tag{39}$$

During the sliding mode and in permanent regime, we have:

$$\sigma(i_{rd}) = 0, \;\; \dot{\sigma}(i_{rd}) = 0, \;\; V_{rd}^{n} = 0$$

Where the equivalent control is:

$$V_{rd}^{eq} = (\dot{i_{rd}^*} + \frac{1}{\sigma T_r} i_{rd} - g\omega_s i_{rq})\sigma L_r \tag{40}$$

Therefore, the correction factor is given by:

$$V_{rd}^{n} = k_{V_{rd}}.sat(\sigma(i_{rd})) \tag{41}$$

$k_{V_{rd}}$: positive constant.

VIII. Simulation Results

The DFIG used in this work is a 4 kW, whose nominal parameters are indicated in appendix.
In order to evaluate the MPPT control strategy proposed in this paper, MATLAB is used to carry out the simulation. We proposed a step change in wind speed is simulated in Fig. 4, the wind speed is start at 5 m per second, at 3 second, the wind speed suddenly become 6 m per second, as 6 second, the wind speed is 7 m per second.

Fig. 5 illustrates the turbine speed curve. We observe after the Fig. 4 and Fig. 5 when wind speed v is 5m/s the optimal turbine speed Ω_t of DFIG is 98.02 rad/s, when v is 6m/s, Ω_t is 111.6 rad/s and when v is 7m/s, Ω_t is 124.3 rad/s, after each adjustment, the stable turbine speed totally with the theoretical value. During this adjusting process, realize the maximum wind energy tracking control.

As can be seen from the Fig. 6, the stator active power injected into the grid is controlled according to the MPPT strategy, when the reactive power is maintained to zero, to guarantee a unity power factor at the stator side as shown in Fig. 7.

Fig. 8 and Fig. 9 present respectively stator and rotor current of the DFIG these show that with the when the wind speed increases the amplitude of stator and rotor current increased.

Fig. 10 presents the power coefficient C_p, it is kept around its optimum value ($C_p = 0.5$) as shown in Fig. 10.

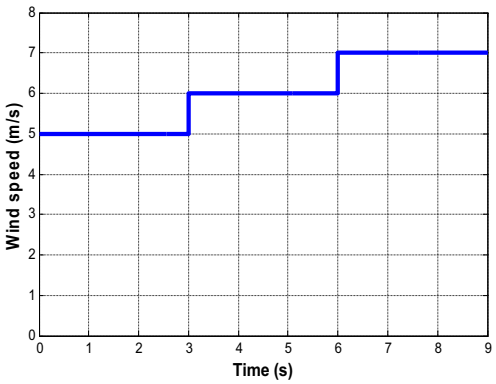

Fig. 4. A step change wind speed profiles

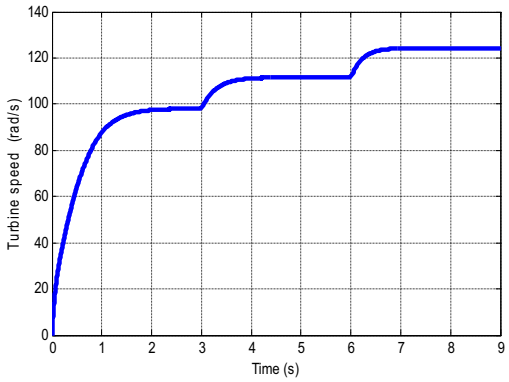

Fig. 5. Turbine speed according the MPPT

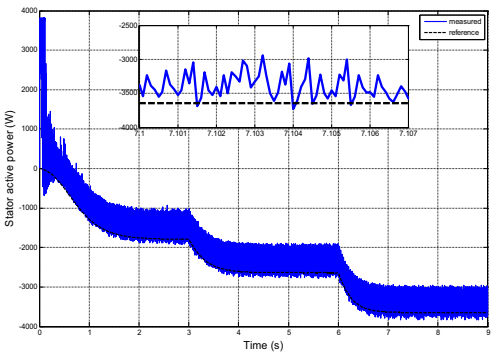

Fig. 6. Stator active power injected in the grid according the MPPT

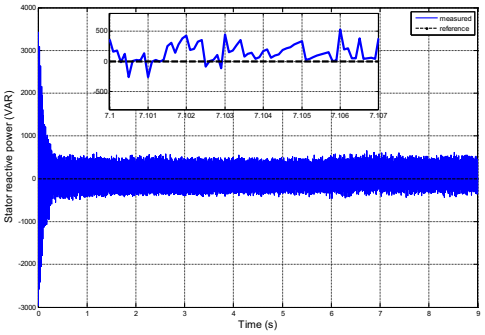

Fig. 7. Stator reactive power

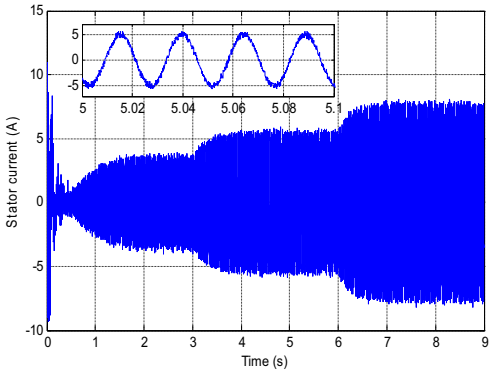

Fig. 8. Phase stator current

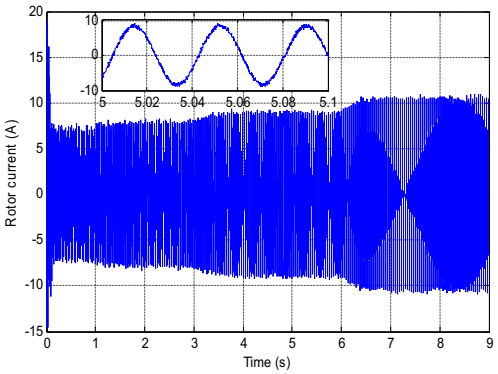

Fig. 9. Phase rotor current

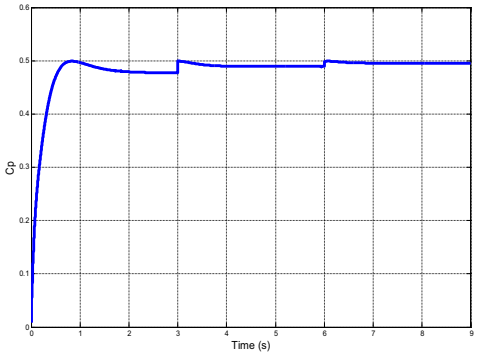

Fig. 10. Power Coefficient C_p variation

IX. Conclusion

In this paper a variable structure control based on a sliding mode control (SMC) of a doubly fed induction generator (DFIG) grid-connected wind energy conversion system, incorporating a maximum power point tracker (MPPT) for dynamic power control has been presented. This structure has been used for reference tracking of active and reactive powers exchanged between the stator and the grid by controlling the rotor converter. Simulation results show good decoupling between stator active and reactive power and good performance obtained in the presence of the variations of wind speed. The obtained results demonstrate that the proposed DFIG system control operating at the variable speed may be considered as an interesting way for problems solution in renewable energy area.

Appendix A
System Parameters

Rated data of the simulated doubly fed induction generator:
Rated values: 4 kW , 220/380 V, 15/8.6 A.
Rated parameters:
$R_s = 1.2(\Omega)$
$R_r = 1.8(\Omega)$
$L_s = 0.1554(H)$
$L_r = 0.1568(H)$
$M = 0.15(H)$
$p = 2$
$J = 0.2(Kg.m^2)$
Wind turbine parameters:
$R = 3(m), G = 5.4.$
Air density : $\rho = 1.22(kg/m^3)$.

Appendix B
Nomenclature

v	wind speed
ρ	air density
R	blade radius
P_m	mechanical power of wind turbine

C_p	power coefficient
S_ω	swept area
λ	tip speed ratio
Ω_t	angular speed of the turbine
C_e	electromagnetic torque
C_r	load torque
J	moment of inertia
β	pitch angle
$V_{sd,q}$	stator $d-q$ frame voltage
$V_{rd,q}$	rotor $d-q$ frame voltage
$i_{sd,q}$	stator $d-q$ frame current
$i_{rd,q}$	rotor $d-q$ frame current
$\phi_{sd,q}$	stator $d-q$ frame flux
$\phi_{rd,q}$	rotor $d-q$ frame flux
R_s	stator resistance
R_r	rotor resistance
L_s	stator inductance
L_r	rotor inductance
M	mutual inductance
σ	leakage factor
p	number of pole pairs
T_s, T_r	statoric and rotoric time-constant
ω_s	stator $d-q$ reference axes speed
ω	rotor $d-q$ reference axes speed
g	slip coefficient.

REFERENCES

[1] M. Verij Kazemi, A. S. Yazdankhah, H. M. Kojabadi, *Direct power control of DFIG based on discrete space vector modulation*, Renewable Energy, Vol. 35, pp. 1033-1042, 2010.

[2] R. Penaa, R. Cardenasb, E. Escobarb, J. Clarec, P. Wheelerc, *Control strategy for a doubly-fed induction generator feeding an unbalanced grid or stand-alone load*, Electric Power Systems Research, Vol. 79, pp. 355-364, 2009.

[3] A. Hazzab, I. K. Bousserhane, M. Kamli, M. Rahli, *Adaptive fuzzy PI-sliding mode controller for induction motor speed control*, International Journal of Emerging Electric Power Systems, Vol. 4, No 1, pp. 1-13, 2005.

[4] X. Zheng, L. Li, D. Xu , J. Platts, *Sliding mode MPPT control of variable speed wind power system*, Power and Energy Engineering Conference, pp. 1-4, APPEEC 2009.

[5] E. S. Abdin, W. Xu, *Control design and dynamic performance analysis of wind turbine-induction generator unit*, IEEE Trans. On Energy Convers., Vol 15, No 1, pp. 91-96, 2000.

[6] A. M. Eltamaly, A. I. Alolah, M. H. Abdel-Rahman, *Modified DFIG control strategy for wind energy applications*, SPEEDAM 2010, International Symposium on Power Electronics, Electrical Drives, Automation and Motion, 2010 IEEE, pp. 659-653, 2010.

[7] M. Machmoum, F. Poitiers, *Sliding mode control of a variable speed wind energy conversion system with DFIG*, International Conference and Exhibition on Ecologic Vehicles and Renewable Energies, MONACO, March 26-29 (2009).

[8] A. Nasri, A. Hazzab, I. K. Bousserhane, S. Hadjiri, P. Sicard, *Two wheel speed robust sliding mode control for electrical vehicle drive*, Serbian Journal of Electrical Engineering, Vol. 5, No. 2, pp. 199-216, November 2008.

[9] Y. Bekakra, D. Ben attous, *A sliding mode speed and flux control of a doubly fed induction machine*, Electrical and Electronics Engineering, 2009, IEEE Conference, pp. I-174 - I-178, 2009.

[10] M. Abid, A. Mansouri, A. Aissaoui, B. Belabbes, *Sliding mode application in position control of an induction machine*, Journal of electrical engineering, Vol. 59, N 6, pp. 322-327, 2008.

[11] J. Lo, Y. Kuo, *Decoupled fuzzy sliding mode control*, IEEE Trans. Fuzzy Syst., Vol. 6, No. 3, pp. 426-435, Aug. 1998.